IMPACT OF SYNCHROTRON RADIATION-INDUCED ENERGY OSCILLATIONS ON SPIN AND BETATRON TUNES IN FFA@CEBAF UPGRADE*

S. Ogur†, S. A. Bogacz, Thomas Jefferson National Accelerator Facility, Newport News, VA, USA
S. Brooks, Brookhaven National Laboratory, Upton, NY, USA
V. Morozov, Oak Ridge National Laboratory, Oak Ridge, TN, USA

Abstract

Jefferson Lab is pursuing an upgrade to nearly double the beam energy of the Continuous Electron Beam Accelerator Facility (CEBAF) to 22 GeV, while maintaining high electron polarization. The upgrade's cornerstone is a new pair of FFA arcs (Fixed Field Alternating Gradient) configured with Halbach style, combined-function permanent magnets, that would support simultaneous transport of additional 6 passes. Beam dynamics in the FFA arc is strongly dominated by synchrotron-radiation effects in both the transverse and longitudinal phase-spaces. As a result, accurate evaluation of polarization transport requires full multi-particle spin–orbit tracking. Preliminary simulations indicate only a small reduction in the polarization magnitude—within the expected 1-σ resolution of typical polarization measurements—yet it reveals substantial changes in the spin orientation when synchrotron radiation is included. In addition to spin tune shifts, the betatron tunes are also notably modified due to radiation-induced energy oscillations. In this report, we present multi-particle tracking studies for the proposed FFA@CEBAF upgrade, focusing on spin transport and tune evolution both with and without synchrotron-radiation effects.

INTRODUCTION

The CEBAF energy-doubling upgrade replaces the two highest-energy recirculation arcs with a pair of Fixed Field Alternating gradient (FFA) arcs based on Halbach-style, combined-function permanent magnets [1–5]. The arcs accept six additional recirculation passes, doubling the CEBAF endpoint energy from 12 to 22 GeV while preserving its key feature: highly polarized continuous-wave electron beams delivered simultaneously to the experimental halls. Because all six passes share the same magnetic field, the higher-energy passes radiate strongly in the combined-function magnets. The resulting synchrotron-radiation (SR) loss and quantum excitation drive correlated energy and orbit oscillations that propagate through the arc optics and feed back into the spin precession; a reliable prediction of the polarization at the experimental halls therefore requires multi-particle spin–orbit tracking with SR included self-consistently. We have launched such a tracking program in Bmad [6] on the baseline FFA FODO lattice [7], with two objectives: (i) quantify the SR-induced depolarization along a 21.55 GeV arc, and (ii) extract the betatron tune shift from the same tracked ensemble.

* This material is based upon work supported by the U.S. DOE, Office of Science, Office of Nuclear Physics contract DE-AC05-06OR23177 and authored in part by UT Battelle, LLC, under Contract No. DE-AC05-00OR22725.
† sogur@jlab.org

DEPOLARIZATION EFFECTS OF SYNCHROTRON RADIATION

At these energies, SR quantum fluctuations dominate over classical-level envelope estimates. We therefore assess SR's impact on the standard 6-D phase space and on the two spin dimensions—via betatron tune shift and depolarization—using multi-particle tracking.

Spin Tune Change due to Synchrotron Radiation

The evolution of the electron spin through the FFA arcs is evaluated using the Bmad accelerator simulation framework, which provides a symplectic treatment of orbital motion together with fully coupled spin tracking. In the magnetostatic environment characteristic of the FFA lattice, the spin motion is governed by the Thomas–Bargmann–Michel–Telegdi (Thomas–BMT) [8] equation

$$\frac{d\vec{S}}{dt} = \vec{\Omega} \times \vec{S}, \tag{1}$$

where the spin precession vector for $\vec{E} = 0$ is

$$\vec{\Omega} = -\frac{e}{m\gamma}\left[(a\gamma + 1)\vec{B}_\perp + (a + 1)\vec{B}_\parallel\right]. \tag{2}$$

Here e and m are the electron charge and mass,

$$a = (g - 2)/2 = 1.159\,652 \times 10^{-3}$$

is the anomalous magnetic moment, and $\vec{B}_\perp$, $\vec{B}_\parallel$ are the magnetic-field components perpendicular and parallel to the particle velocity, in the form used internally by Bmad for purely magnetic elements. At $E = 21.55$ GeV the Lorentz factor is $\gamma = E/m_e c^2 \approx 4.220 \times 10^4$, and the spin tune in a purely magnetic system is

$$\nu_s = a\gamma \approx 48.9. \tag{3}$$

The physically relevant quantity is the spin precession angle per 180 degree arc pass,

$$\theta_s = \pi\nu_s = \pi a\gamma \approx 154 \text{ rad}, \tag{4}$$

i.e. nearly 24.4 full 2π rotations during a single recirculation arc. In terms of path length s [8]:

$$\frac{d\vec{S}}{ds} = \frac{1}{v}\vec{\Omega} \times \vec{S}, \tag{5}$$

with $\vec{\Omega}$ from Eq. (2); radial excursions in the FFA magnets modulate the local spin-precession rate. For CEBAF-style recirculation, the cumulative spin evolution is the sum of arc-by-arc Thomas–BMT precessions; BMAD performs the tracking pass-by-pass. For each particle, BMAD returns $\vec{S}_i(s)$ and the instantaneous polarization. At 21.55 GeV, SR becomes dominant and acts both on the orientation and the magnitude of the polarization,

$$P = \sqrt{\langle S_x \rangle^2 + \langle S_y \rangle^2 + \langle S_z \rangle^2}, \qquad (6)$$

with $\Delta P = P_{\text{final}} - P_{\text{initial}}$.

Betatron Tune Change due to Synchrotron Radiation

The horizontal betatron tune Q_x counts the transverse oscillations per lattice section and is related to the phase advance $\Delta\mu_x$ in normalized phase space by $Q_x = \Delta\mu_x/(2\pi)$. For a tracked ensemble, the entrance and exit horizontal phase-space coordinates are written in complex form

$$z_i = X_i + iP_{X,i}, \qquad z_f = X_f + iP_{X,f}, \qquad (7)$$

with the Courant–Snyder normalized coordinates

$$X = \frac{x}{\sqrt{\beta_x}}, \qquad P_X = \sqrt{\beta_x}\, p_x + \frac{\alpha_x}{\sqrt{\beta_x}}\, x, \qquad (8)$$

and β_x, α_x the Twiss parameters at each location. In normalized phase space, particle motion is a pure rotation, with $|z|$ the Courant–Snyder invariant amplitude and $\arg(z)$ the betatron phase. To isolate the oscillatory motion the centroid is subtracted, $z'_{i,j} = z_{i,j} - \langle z_i \rangle$ and $z'_{f,j} = z_{f,j} - \langle z_f \rangle$, and the ensemble-averaged phase advance follows from the argument of the complex inner product

$$\Delta\mu_x = \arg\left(\sum_j z'^{*}_{i,j}\, z'_{f,j}\right), \qquad Q_x = \frac{\Delta\mu_x}{2\pi}. \qquad (9)$$

In the linear approximation, the transport in normalized phase space reduces to a pure rotation,

$$\begin{pmatrix} X_f \\ P_{X,f} \end{pmatrix} = R(\mu) \begin{pmatrix} X_i \\ P_{X,i} \end{pmatrix}, \quad R(\mu) = \begin{pmatrix} \cos\mu & \sin\mu \\ -\sin\mu & \cos\mu \end{pmatrix}, \qquad (10)$$

with $\mu = 2\pi Q_x$, so the method directly extracts this rotation angle from the tracked ensemble without explicit matrix reconstruction.

LATTICE AND INITIAL BEAM

We track $N = 10^4$ macroparticles through a 75-cell FFA arc. At the sixth-pass energy of 21.55 GeV, the arc sustains a synchrotron-radiation energy loss of ~182 MeV per pass, computed from BMAD's radiation-integral output for the FFA arc lattice. This estimate is restricted to the arc proper; SR losses in the spreaders, recombiners, and other beamline sections will be incorporated in future start-to-end simulations. The initial 6-D Gaussian distribution follows the FFA emittance budget. The longitudinal path-length expansion is captured up to third order,

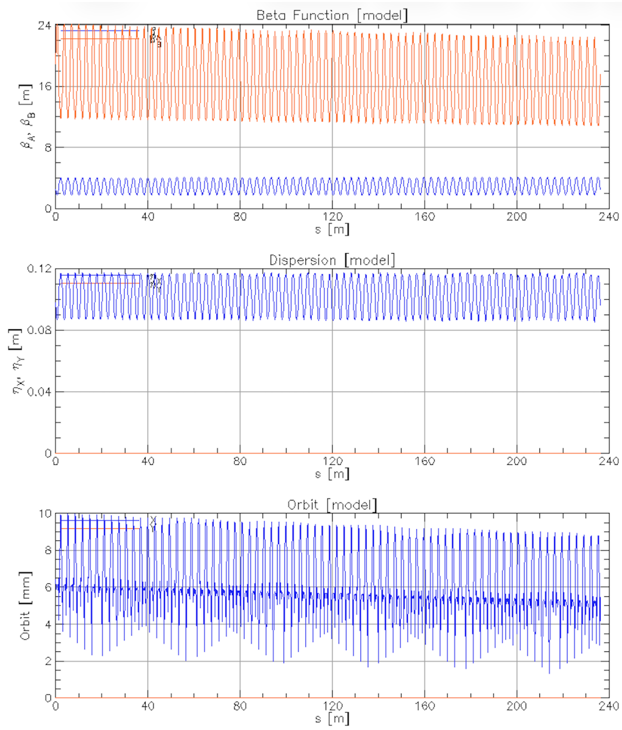

Figure 1: Periodic optics of the 21.55 GeV FFA East arc, SR ON. Top: $\beta_{x,y}$. Middle: dispersion. Bottom: closed orbit.

$$\Delta L(\delta) = R_{56}\,\delta + T_{566}\,\delta^2 + U_{5666}\,\delta^3, \qquad (11)$$

which is essential to reproduce the energy-oscillation amplitude when SR is on. Each particle carries a unit spin; spin tracking is performed under (a) SR loss and oscillations OFF and (b) SR loss and oscillations ON. A Wien-filter spin-rotation device will be installed in the new LERF injector to deliver longitudinally polarized beam to the halls; the initial spin orientation chosen here is purely illustrative ($s_x = -0.9$ at injection so that $s_z \simeq +0.9$ at the arc exit). Figure 1 shows the periodic Twiss functions, dispersion and closed orbit of the 21.55 GeV (sixth-pass) FFA arc with SR ON. The optics is intentionally non-closed: $\eta_x \approx 9$–11 cm and an off-axis closed orbit of ~ 5–8 mm allow all six passes to share the same magnets. The injected 6-D Gaussian distribution shown in Fig. 2 carries a finite horizontal centroid and slope inherited from the open-geometry dispersion; the vertical plane is nominally matched and the longitudinal plane is uncorrelated.

SPIN TRANSPORT RESULTS

Without Synchrotron Radiation

With SR OFF the beam exits the arc with the spin distribution shown in Fig. 3: $\langle s_z \rangle = 0.82127 \pm 0.00002$ and $\sigma_{s_z} = 1.8 \times 10^{-3}$, with a polarization-magnitude change $\Delta|S| = 1.15 \times 10^{-5}$, confirming that the deterministic spin transport is intrinsically very benign.

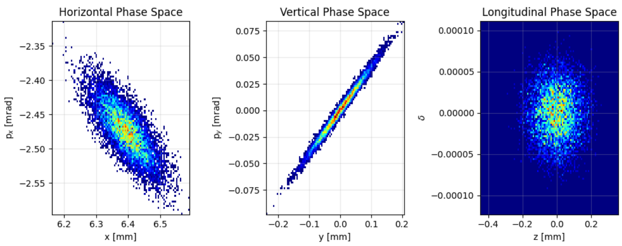

Figure 2: Initial 6-D phase-space distribution at the arc entrance: horizontal (x, p_x), vertical (y, p_y), longitudinal (z, δ).

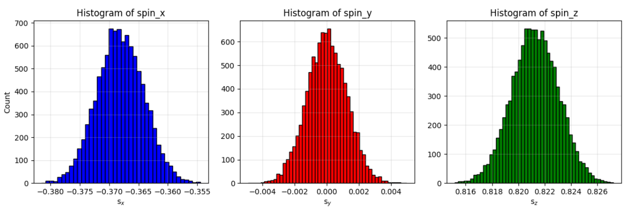

Figure 3: Final spin distribution at the arc exit, SR OFF. $\langle s_z \rangle = 0.82127 \pm 0.00002$, $\sigma_{s_z} = 1.8 \times 10^{-3}$, $\Delta|S| = 1.15 \times 10^{-5}$.

With Synchrotron Radiation

Switching SR loss and stochastic oscillations ON dramatically alters the spin orientation, Fig. 4. The mean longitudinal spin shifts to $\langle s_z \rangle = 0.88125 \pm 0.00007$ and the spread grows to $\sigma_{s_z} = 7.0 \times 10^{-3}$. The polarization-magnitude change increases to $\Delta|S| = 7.8 \times 10^{-4}$, still well within the 1σ resolution of typical Compton, Møller and Mott polarimeters at CEBAF [9] at all CEBAF operational energies, but the rotation of the mean spin would manifest as a measurable systematic offset if uncorrected. The interpretation is that SR-induced stochastic energy oscillations, amplified by the non-zero η_x and T_{566}, U_{5666}, modulate the local spin tune $a\gamma$ along each particle's trajectory.

BETATRON TUNE EVOLUTION

The same tracked ensemble allows a self-consistent extraction of the betatron tune via Eq. (9). Without SR, the nominal arc tune $(Q_x, Q_y) = (14.0787, 2.3222)$ is recovered to $\lesssim 10^{-3}$ by the normalized-phase-space estimator. With SR ON the Bmad optics report yields $(Q_x, Q_y) = (14.1272, 2.4193)$, i.e. a shift of $\Delta Q_x \simeq +0.05$, $\Delta Q_y \simeq +0.10$ driven by the combination of the SR-induced energy oscillation and the chromaticity of the open-geometry FFA cell. The tracked ensemble also shows a 0.8 mm orbit shift and 0.3 mrad angular shift in the horizontal plane, together with a modification of the Twiss parameters ($\beta_x : 2.495 \longrightarrow 3.830$ m, $\alpha_x : 1.192 \rightarrow 1.344$, $\gamma_x : 0.970 \rightarrow 0.925$, $\varepsilon_x : 1.264 \rightarrow 2.213$ nm), indicating a modest mismatch that should be corrected in the arc-to-Linac matching. The corresponding normalized phase-space ensemble at the entrance and exit of the arc is shown in Fig. 5. Fitting the centroid-subtracted complex inner product of Eq. (9) to this ensemble gives a normalized phase advance of $\Delta\mu = -0.7998$ rad, equivalent to $Q_x = -0.12729$ (mod 1) per arc, in agreement with the

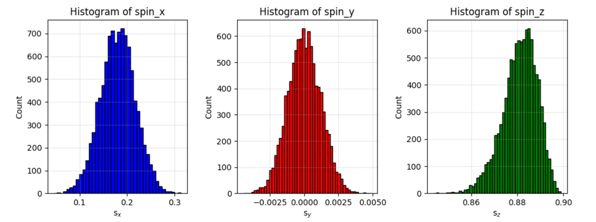

Figure 4: Final spin distribution at the arc exit, SR ON. $\langle s_z \rangle = 0.88125 \pm 0.00007$, $\sigma_{s_z} = 7.0 \times 10^{-3}$, $\Delta|S| = 7.8 \times 10^{-4}$. Although $|S|$ barely changes, the spin orientation is rotated significantly relative to the SR-OFF case.

Bmad-predicted shift $\Delta Q_x \simeq +0.05$ relative to the SR-OFF lattice. The corresponding raw (un-normalized) complex-phase fit yields $\Delta\mu_{\text{raw}} = -0.5365$ rad ($Q_x = -0.0853$), the $\sim$30% disagreement reflecting the mismatch in the entrance and exit Twiss parameters: the raw estimate is biased by the change in β_x and α_x between the two locations, whereas the normalized estimator removes this bias by construction.

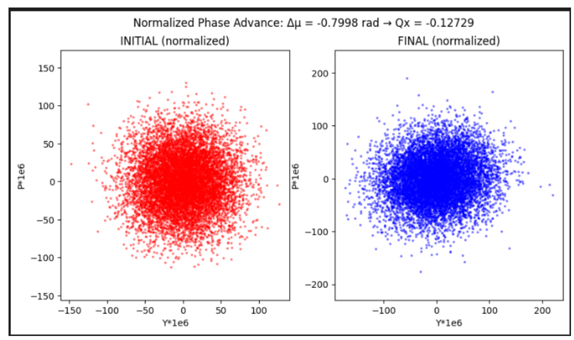

Figure 5: Normalized horizontal phase-space distribution at the entrance (red) and exit (blue) of the 21.55 GeV FFA arc with SR ON. The centroid-subtracted complex inner product yields the per-arc phase advance $\Delta\mu = -0.7998$ rad ($Q_x = -0.12729$ mod 1).

CONCLUSIONS AND OUTLOOK

The FFA@CEBAF arcs operate in a regime where SR distorts both spin and orbital optics while keeping $|S|$ within the 1σ resolution of standard CEBAF polarimeters. The dominant effects per 180 degree arc pass are a coherent rotation of the mean spin ($\Delta s_z \sim 6 \times 10^{-2}$), a tune shift $\Delta Q_x \simeq +0.05$, $\Delta Q_y \simeq +0.10$, and a 0.8 mm/0.3 mrad centroid shift with a $\sim$50% change of β_x. The spin rotation must be folded back into the source Wien-filter setting and the tune/Twiss perturbation absorbed by the arc-to-Linac matching. Future work will benchmark Bmad against Zgoubi [10] and extend the model start-to-end [2].

REFERENCES

[1] A. Bogacz *et al.*, "20-24 GeV FFA CEBAF Energy Upgrade", in *Proc. IPAC'21*, Campinas, SP, Brazil, paper MOPAB216, doi:10.18429/JACoW-IPAC2021-MOPAB216

[2] S. Ogur *et al.*, "Status of 22 GeV CEBAF upgrade using FFA arcs", presented at IPAC'26, Deauville, France, 2026, paper THP3304, this conference.

[3] S. Ogur *et al.*, “FFA beam transport demonstration development for the CEBAF 22 GeV upgrade”, presented at IPAC’26, Deauville, France, 2026, paper THP3305, this conference.

[4] J. Benesch, “Variations on the 104 mm quad for FFA and other uses”, JLAB-TN-23-018, 2023, https://jlabdoc.jlab.org/docushare/dsweb/Get/Document-289443/23-018.pdf

[5] J. Benesch, “104 mm gap arc-zero dipoles for positrons and FFA”, JLAB-TN-24-039, 2024, https://jlabdoc.jlab.org/docushare/dsweb/Get/Document-289443/24-039.pdf

[6] D. Sagan, “Bmad: A relativistic charged particle simulation library”, *Nucl. Instrum. Meth. A*, vol. 558, pp. 356–359, 2006, doi:10.1016/j.nima.2005.11.001

[7] R. Bodenstein, “FFA at CEBAF lattice”, branch FFA_Arc_Update, https://github.com/RyanBodenstein/FFA_at_CEBAF

[8] B. W. Montague, “Polarized Beams in High Energy Storage Rings”, *Phys. Rep.*, vol. 113, pp. 1–96, 1984, doi:10.1016/0370-1573(84)90031-0.

[9] J.A. Magee *et al.*, “A novel comparison of Møller and Compton electron-beam polarimeters”, *Phys. Lett. B*, vol. 766, pp. 339–344, 2017, doi:10.1016/j.physletb.2017.01.026

[10] F. Méot, “The ray-tracing code Zgoubi—status,” *Nucl. Instrum. Meth. A*, vol. 767, pp. 112–125, 2014, doi:10.1016/j.nima.2014.07.022